Materials & Design 222 (2022) 111104

Contents lists available at ScienceDirect

Materials & Design

journal homepage: www.elsevier.com/locate/matdes

Extensional rheology of battery electrode slurries with water-based binders

C.D. Reynolds [a,b,*], J. Lam [a,b], L. Yang [a], E. Kendrick [a,b]

[a] School of Metallurgy and Materials, The University of Birmingham, Edgbaston, Birmingham B15 2SE, UK
[b] Faraday Institution, Campus, Quad One Becquerel Avenue Harwell, Didcot OX11 0RA, UK

HIGHLIGHTS

- Extensional rheology of battery electrode slurries is quantified.
- Extensional properties are shown to vary signicantly between formulations.
- Branched polymer binder dramatically alters slurry behaviour in extension.
- Slurry behaviour under extension cannot be predicted from shear.
- Extension is a key parameter for understanding and modelling battery manufacturing.

GRAPHICAL ABSTRACT

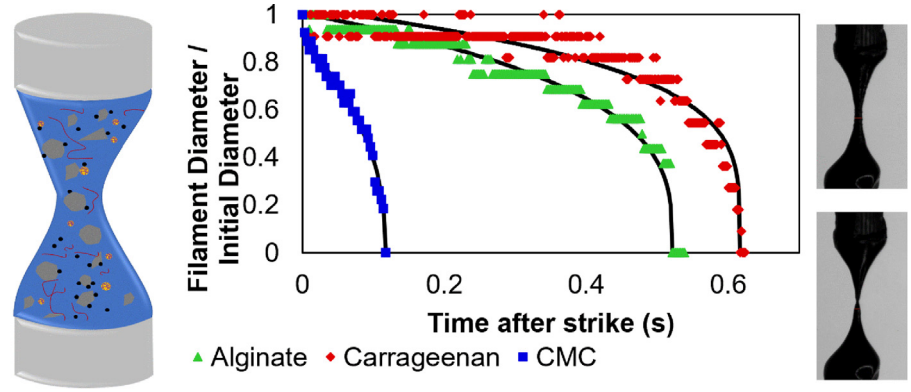

ARTICLE INFO

Article history:
Received 5 April 2022
Revised 20 August 2022
Accepted 26 August 2022
Available online 30 August 2022

Keywords:
Extensional rheology
Electrode slurry
Battery manufacturing
Sustainable binders
Metrology

ABSTRACT

Precise rheological properties of inks and slurries are essential to providing homogeneous, well controlled and reproducible coatings, particularly in electrode manufacturing for batteries. The rheology can aid understanding of the slurry structure, as well as optimisation of the process conditions to create electrode coatings with the desired microstructure. The shear rheology is typically measured, however the mixing and coating steps contain significant extensional flows, this omits a significant part of the rheological response. Here the extensional properties of battery electrode slurries are quantified using a miniature extensional rheometer. This requires tiny samples (<1 ml) and provides rapid capture of the extensional properties, allowing easy repetition. The extensional behaviour varies significantly between different formulations and binder systems. The additional extensional rheometry measurements are key for understanding flow in a coater and the underlying slurry structure, and are not predicted by shear rheology. This novel extensional rheology technique, applied to battery electrode slurries, provides key rheological parameters, rapidly, and is essential to understanding the precise rheological properties and control for coating depositions.

1. Introduction

Scale up of battery manufacturing is a current global challenge as we shift from petrol and diesel towards electric vehicles [1]. There is also an intensified focus on finding novel battery materials and developing manufacturing processes, which improve the

* Corresponding author.
E-mail address: c.d.reynolds@bham.ac.uk (C.D. Reynolds).

https://doi.org/10.1016/j.matdes.2022.111104
0264-1275/

energy and power density of batteries, reduce reliance on critical raw materials, and improve recyclability [2,3]. To enable adoption of these new technologies, and support rapid expansion into manufacturing, these manufacturing process must be well understood, allowing fast optimisation with wide process windows. Optimisation of the processes when establishing a new manufacturing line, or formulation on an existing line, is costly and time-consuming, typically performed by trial and error with large matrices of experiments, which determine parameters specific to the setup used. Understanding of the manufacturing process and the physics of the mixing and coating processes in greater fundamental detail, will reduce time to production through modelling and digital twins of the process. This paves the way for rapid development of battery technologies [4,5].

Battery manufacturing is a complex process with multiple steps, active materials, conductive additives and polymeric binders are mixed into a slurry, then coated onto a metallic current collector, dried and calendared (compressed) to produce the electrode [5]. An enormous range of parameters and properties can be varied, and measured at each stage [5]. There are currently limited metrology options that can be used to characterise the starting materials, electrode slurry, and electrode coating. Significantly more techniques are required to elucidate the mechanisms and interactions of the components which occur at each stage of the manufacturing process, and ultimately provide a predictive understanding of the process [4]. One key aspect of this is characterisation of the slurry rheology. This is vital as it dictates the flow in the coater, and has significant impact on the final coating microstructure [6].

To fully describe the complex flow during coating, both shear and extensional components are needed, thus slurry behaviour in both these flows must be understood. The most common coater used industrially is the slot die coater, which has significant extensional flow [7,8] as the slurry exits the head (Fig. 1). In research settings, blade and comma bar coaters are commonly used, which also have significant extension flow (e.g. for coating of Newtonian fluid with a blade angle of 45° the shear and extension rate is equal [7]). However, currently only the shear rheology of slurries is routinely measured.

These geometries are similar to those encountered in polymer processing, where many processing flows (e.g. extrusion, film casting) are known to be extensional in nature, and shear properties alone are not enough to evaluate the behaviour in these flows [9]. For example, extensional rheology is key to understanding die swell of polymers from a capillary [10], a setup similar to the head of a slot die coater, so the extensional properties of the slurry will likely dictate the expansion of slurry at the die head, as well as expansion of the slurry after passing through the gap in a blade or comma bar coater.

Electrode slurries are known to be viscoelastic and their rheology is highly sensitive to the ratios of components [11,12], and key to the final coating microstructure [6]. Because of the extensional flows involved in coating, it is highly likely extensional rheology is also a key factor determining coating microstructure. As polymers are known to have complex extensional behaviour, the polymeric binder is likely to be key to the extensional properties of the slurry. Extension could therefore be a key tool in design of new slurries, and final coating microstructures for the next generation of batteries.

There are several methods for quantifying extensional flow, which could be applied to electrode slurries. Filament stretching rheometers [13,14], place the sample between two plates and subjects it to an extensional strike, moving the plates apart and observing the filament diameter and force on the filament over time. This typically requires complex setups to measure the forces involved and calculate the stress on the filament. Capillary thinning is a similar technique, but uses strike conditions which leave a filament between the plates, which then thins under gravity, a known force, so the extensional properties can be extracted from the filament diameter alone. This was commercialised in the capillary breakup extensional rheometer (CaBER) [15,16] and has been extended to faster strike times in the Cambridge Trimaster [17]. While these are simpler setups, there also exists a design for a miniaturised filament thinning rheometer, Seymour [18,19], which uses the capillary thinning principle but was designed to be low cost, transportable and require a tiny amount of sample. Here this technique is applied as it is fast, low cost and could be rapidly adopted in industrial settings, where additional metrology is vital for process understanding, modelling and quality control.

The extracted filament profiles can be compared directly, and models can be fit to extract rheological parameters. Multiple models for filament thinning exist depending on the fluid behaviour, the most common being Newtonian, which exhibits a linear decrease in diameter over time, elastic fluids show initial thinning which slows over time [20], and yield stress fluids which have an initial plateau before thinning [21]. Models for these fluid types are comprehensively summarised by McKinley [22].

This study examines the extensional properties of electrode slurries, using a hard carbon anode as a test system, replacing the polymeric binder to examine the effect on extensional properties. These are fit with models to classify their extensional behaviour and provide parameters for comparison of slurries. Shear rheology is also quantified to show shear alone is not sufficient to predict extensional behaviour. By demonstrating the impact for-

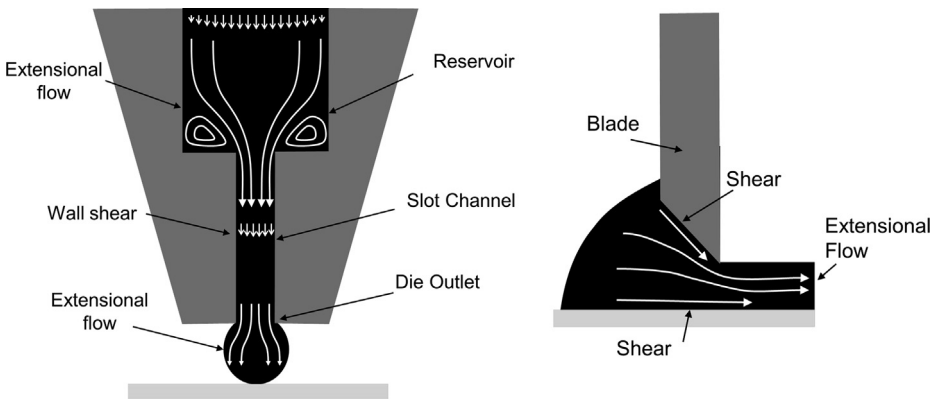

Fig. 1. (left) Illustration of flow in a slot die coater showing significant extensional components (note that flow evolves at the die outlet over time, becoming more complex) (right) illustration of flow and extensional components in blade coating.

mulation can have on these properties, their importance is demonstrated, as well as paths to design formulations with specific extensional properties.

2. Methods

2.1. Materials

Hard Carbon was Kuraray Kuranode Type 1. Carbon black was Imerys TIMCAL Super C65. Carboxy Methyl Cellulose (CMC) was Ashland BVH8. Styrene Butadiene Rubber (SBR) was Zeon BM451-B. Sodium Alginate was sourced from Sigma Aldrich. Iota-Carrageenan was sourced from Fisher (AAJ6060322). Guar gum was sourced from Sigma Aldrich (G4129).

2.2. Slurry preparation

The formulation of solids in the slurry was (by weight percentage) 92:3:5 hard carbon: binder: carbon black. For CMC:SBR the ratio was 1:2. These were made up to 49.5 wt% in water.

100 g of slurry was prepared using an Intertronics THINKY mixer. The binder (CMC, Alginate, Carrageenan, Guar) was pre-dispersed in the full amount of water in three intervals, each 1 min at 500 rpm, followed by 10 min at 2000 rpm. Half of this was used to pre-disperse the carbon black, mixed for 1 min at 500 rpm, and 5 min at 2000 rpm. The hard carbon and final half of binder solution was added before undergoing a further mix for 1 min at 500 rpm, and 10 min at 2000 rpm mix and a degas step of 2200 rpm for 3 min. For CMC/SBR the SBR was added at the end before a final slower mix at 500 rpm for 5 min – the other slurries underwent this mix without addition to keep the procedure consistent.

2.3. Shear rheology measurements

Viscosity measurements were conducted on a Netzsch Kinexus Pro + rheometer equipped with a Peltier plate and a 40 mm diameter rough plate with a gap of 1 mm. Samples were equilibrated at 25 °C for 5 min before testing in the shear rate range between 0.01 and 250 s^{-1}.

2.4. Surface tension measurements

Surface tension measurements were conducted using a Dyne Sigma 703D tensiometer, using the Wilhelmy plate method. The plate was lowered just below the surface of the slurry, retracted and then the instrument zeroed. The plate was then lowered into the slurry and retracted so it was as close to the surface as possible, where the surface tension was allowed to stabilise, and recorded. This was repeated 3 times and averaged.

2.5. Extensional measurements

The 3D printed Seymour extensional rheometer was used, with 1.9 mm top and bottom plates. The starting and final positions of the plates was adjusted, as specified in Table 1. The sample was loaded in between the plates and the solenoid switched on (producing a fast motion of the top plate, strike times given in Table 1). This was imaged using a high speed USB 3.0 camera, at ~ 300 fps. The filament diameters at the midpoint of the plates over time were extracted from the recorded videos using in-house MATLAB code.

3. Results and discussion

Hard carbon anodes were chosen as a test system, which are a promising technology for both lithium and sodium ion batteries [23] and can be dropped into existing lithium-ion manufacturing lines. The binder system was varied between formulations, changing the standard Carboxymethylcellulose (CMC) and styrene butadiene rubber (SBR) (combined referred to as CMC) for other water-based binders, Iota-Carrageenan (Carrageenan), Sodium Alginate (Alginate) and Guar gum (Guar). These have the potential advantage of removing the need for the oil-based binder SBR, which adds flexibility needed to prevent cracking and delamination of the coating. Removing SBR from the formulation would allow for more sustainable manufacturing, as well as a simplified mixing process.

A consistent mixing protocol was utilised (see methods) and the surface tension and shear rheology was characterised. The slurries were then characterised using a 3D printed Seymour rheometer [18,19]. The slurry is sandwiched in-between two plates which are rapidly moved apart using a solenoid, creating a filament that thins under gravity (Fig. 2). The filament is imaged using a high-speed camera and an in-house MATLAB code used to extract the filament diameter over time. The starting and ending position of the top plate was varied, and experiments which produced similar filament diameters compared for each slurry (in the range 0.17 to 0.28 mm).

3.1. Changing binder system

In the shear rheology (Fig. 3), the magnitude of the viscosity changes between formulations, but all demonstrate a similar shear thinning responses. There is seen a change in gradient for the slurries at around 1 s^{-1}, Guar shows a slight decrease in gradient, where the other slurries show an increase, most noticeably for CMC and alginate. The lack of zero shear viscosity indicates a yield stress for all slurries. CMC shows the lowest viscosity and the curves shift upwards in the order CMC, alginate, carrageenan, guar. The CMC/SBR is expected to have lower viscosity as the SBR contributes little to the rheology of the slurry, so the CMC alone is at lower weight percentage (1%) vs the other biopolymers. These were chosen for comparison as the other biopolymers are potential alternatives to remove the SBR, so could be used in new formulations at 3%, the combined weight fraction of CMC and SBR, without reducing the fraction of active material.

The slurries were also examined in oscillatory shear (Fig. 4). Here a similar trend is observed, all slurries demonstrated elastic behaviour (with elastic modulus $G' > G''$) except CMC, which showed $G' < G''$ at all the frequencies measured. While Guar and carrageenan showed very similar elastic moduli, the viscous modulus of carrageenan was signicantly lower, indicating a more elastic slurry.

In extension, there is a notable difference between the thinning profiles of the different binder systems (Fig. 5). The CMC binder system is closest to Newtonian behaviour, showing a mostly linear profile, however the increase in the rate of thinning immediately before breakup hints at yield stress behaviour, as observed in shear.

Alginate and Carrageenan binders both show similar times to breakup, but the Carrageenan demonstrates a small initial plateau-like region until intermediate times where the Alginate, like the CMC, shows a uniform thinning with an increase in rate near the end. Guar shows a much longer initial region and hence a much higher time to breakup, suggesting a much higher resistance to extensional flow than the other binder systems.

The influence of binder volume fraction upon the extensional rheometry response was considered. The density of alginate is low-

Table 1
Experimental and fitting parameters for models applied to the thinning of each slurry and their shear rheology.

		Slurry Binder			
		CMC/SBR	Alginate	Carrageenan	Guar
Model Parameters	**Surface Tension (mN/m)**	51.28	53.92	54.70	43.63
	Starting Plate Separation (mm)	0.81	1.18	0.98	0.72
	Final Plate Separation (mm)	2.59	4.98	5.75	5.04
	Strike Time (s)	0.006	0.005	0.005	0.007
Newtonian	**Viscosity, n_s (Pa.s)**	2.22	22.46	46.71	234.74
$\frac{R_{mid}(t)}{R_0} = 0.0709\frac{\sigma}{\eta_s R_0}(t_c - t)t_c = 14.1\frac{\eta_s R_0}{\sigma}$	**Starting radius, R_o (mm)**	0.27	0.19	0.18	0.18
	Critical Time to breakup, t_c	0.17	1.12	2.17	13.56
Bingham Plastic	**Yielding Radius, Ry (mm)**	0.24	0.18	0.16	0.12
$\frac{R_{mid}(t)}{R_0} = \frac{\frac{\sigma}{R_0}}{\tau_y\sqrt{3}}\left(1 - exp\left(\frac{\tau_y(t-t_c)}{2\mu\sqrt{3}}\right)\right)\tau_y = R_y\frac{\sigma}{\sqrt{3}}$	**Dynamic Viscosity, mu (Pa.s)**	1.33	6.05	3.69	10.66
Power Law	**Power Law Index, n**	0.43	0.30	0.23	0.16
$\frac{R_{mid}(t)}{R_0} = \phi(n)\frac{\sigma}{K}(t_c - t)^n\phi\ \frac{2^{-n}}{3}$	**Consistency Factor, K (N/m.s)**	0.00	0.00	0.00	0.00
	Critical Time to breakup, tc	0.12	0.52	0.62	7.77
Shear Rheology (Power Law)	**K Low Shear Rate**	20.29	100.62	482.35	798.74
	n Low Shear Rate	0.07	0.21	0.05	0.22
$Stress = K(ShearRate)^n$	**K High Shear Rate**	10.18	74.05	423.02	770.99
	n High Shear Rate	0.62	0.44	0.18	0.10

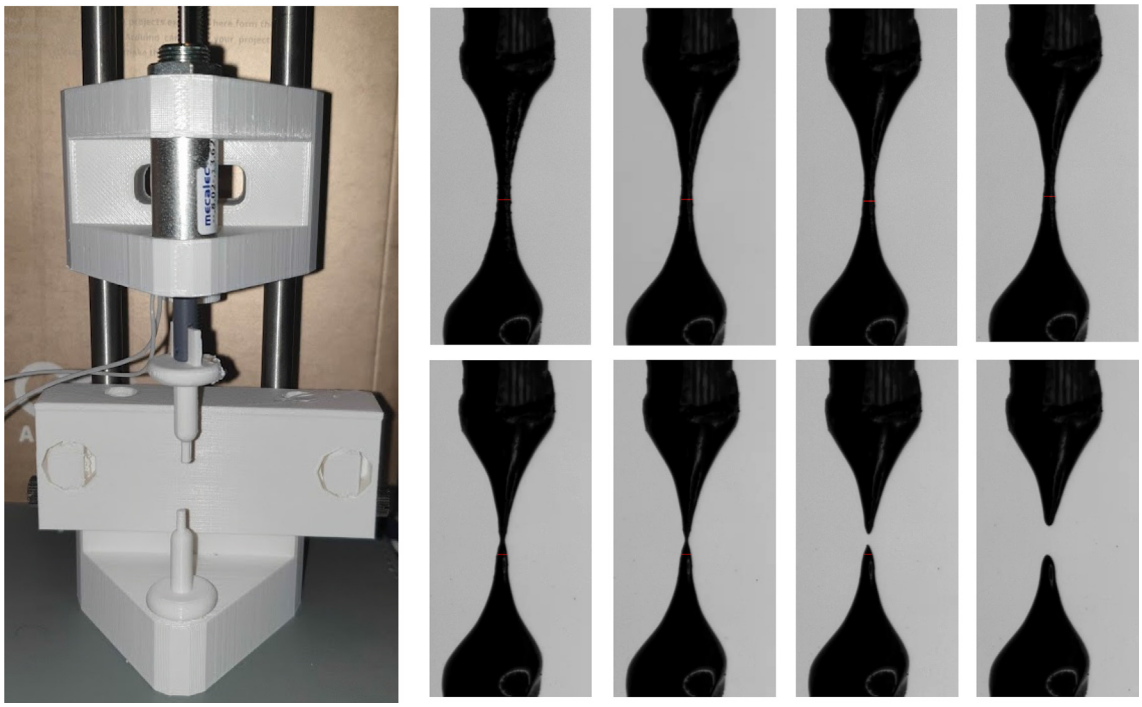

Fig. 2. (left) 3D printed Seymour rheometer (right) example images of filament thinning.

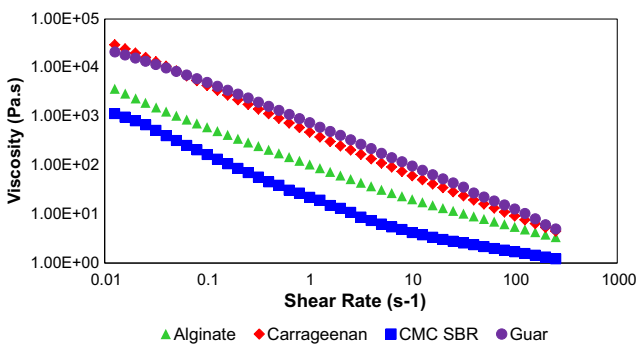

Fig. 3. Steady shear rheology of hard carbon slurries with different binders.

est at 1.1 g/cm^3 where Carrageenan has a higher density of 1.37 g/cm^3 and Guar higher still at 1.6 g/cm^3. As they were all added at the same weight percentage, the higher density polymers have lower volume fraction in solution and hence are expected to have lower viscosity. However, the opposite trend is seen between Alginate, Guar and Carrageenan for our materials, suggesting this is not the dominant effect. Despite CMC having a high density of 1.6 g/cm^3, SBR (density 0.96 g/cm^3) is also included in the binder fraction, and when this is included, their average density is 1.16 g/cm^3. Hence again it would be expected to have a higher viscosity if volume fraction was the determining factor, which is not the case.

Drying of the slurry can be considered negligible as the experiments were all < 10 s, the room temperature was in the range 20–

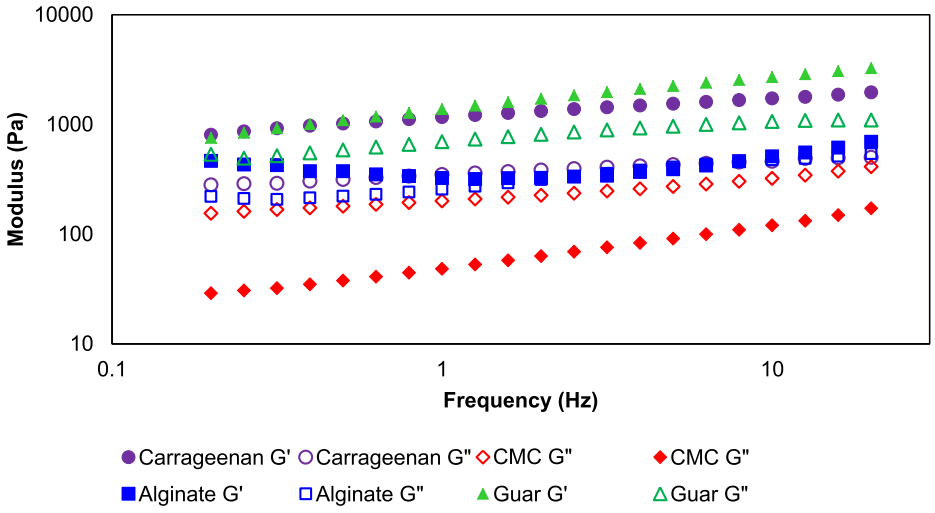

Fig. 4. Oscillatory Shear frequency sweeps of hard carbon slurries with different binders.

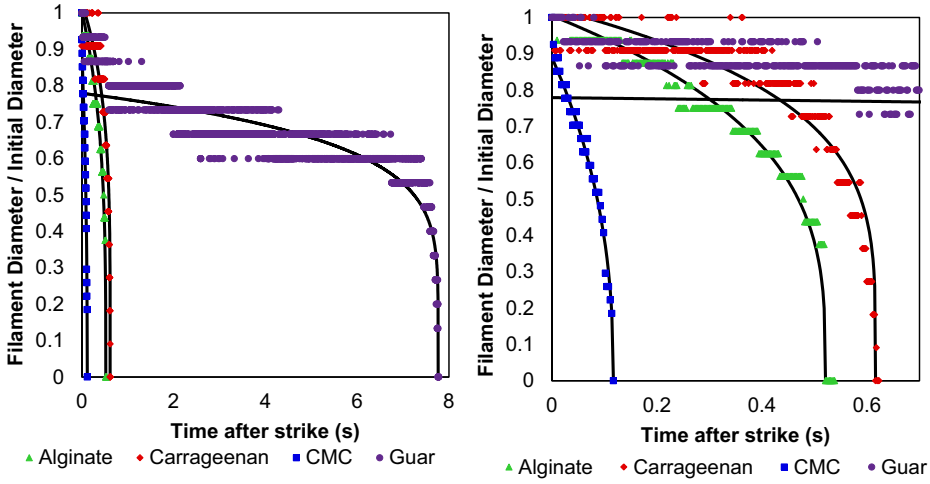

Fig. 5. (left) Filament thinning data for each slurry, lines show fits with 1D Power Law, (right) zoomed in on shorter times.

22 °C and no drying was observed in the bulk slurry. While the filaments produced had very small volumes, which could dry quickly, the data does not support the presence of drying during the experiment. For the Guar system, higher viscosity may be expected to slow solvent escape and thus drying, but also extend the experiment, leading to more time to dry. However, the plateau-like region began at short times (<1 s), and the other systems (including carrageenan which has a similar viscosity in shear) did not exhibit this behaviour in this region (in fact it is around this time that their thinning rates increased, and the filaments broke). Hence the long initial region observed for Guar was not due to filament drying.

Of the binders used, Guar gum is the only branched polymer, where CMC, Carrageenan and Alginate are linear [24]. The inclusion of branch points significantly increases extensional viscosity and extensional hardening over linear polymers and hence this is likely the reason Guar stands out signicantly in the extensional measurements, despite having similar behaviour in shear. Extensional rheology is therefore a useful tool to probe the presence of branched polymers in electrode slurries, and addition of branched binders could be a useful tool to tailor the extensional properties.

3.2. Modelling the filament thinning profiles

The filament thinning data were fit to 3 models for filament thinning, Newtonian, Power Law (1 Dimensional) and Bingham Plastic. The Newtonian model assumes a linear relationship between shear rate and shear stress, and the Bingham plastic adds to this a yield stress, a minimum stress required for the material to flow, above which the material behaves as Newtonian. Power law materials have a non-linear relationship between shear stress and rate and are 'pseudoplastic' when $0 < n < 1$, i.e. they flow instantaneously with shear without a yield stress, but viscosity decreases with shear rate. Despite the observed differences in behaviour, the power law model provided the best fits (by least squares) for all the samples. However, all 3 models gave reasonable fits, but Newtonian could not capture the increase in thinning rate near filament break up. (Fig. 6).

The trends in the parameters extracted (Table 1) follow the same pattern in each case. As seen in the shear rheology, the viscosity increases in the order: CMC, Alginate, Carrageenan, Guar. This same pattern is seen in the viscosity extracted from the Newtonian model, the dynamic viscosity extracted from the Bingham model and the consistency index fitted in the Power Law model. The Bingham fits also fit a critical radius for the onset of capillary

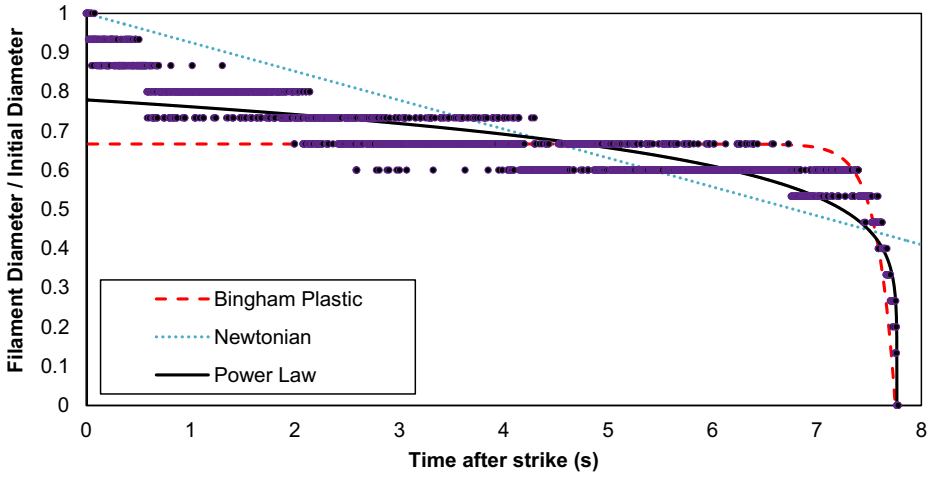

Fig. 6. Comparison of Power Law, Bingham Plastic and Newtonian models for thinning for Guar slurry.

driven thinning, which is seen to decrease in the same order, indicating a higher yield stress. In the Power Law fits, a flow behaviour index n is also extracted, which is <0.5 for all samples, indicating significant pseudo plastic behaviour. This decreases in the sample pattern across the samples, indicating a increase in the pseudo-plastic behaviour between the formulations.

The significant result is that these extensional results, which are important for processing and handling (e.g. the Guar-based slurry formed long strands when handled), cannot be predicted by the shear rheology. The Guar and Carrageenan slurries appear remarkably similar in shear, but distinctly different in extension.

The shear rheology was fit with a power law to compare to the extracted extensional parameters. Two fits were necessary to capture the low shear (0.01 – 1 s^{-1}) and high shear (1 s^{-1} –1000 s^{-1} regions), due to the shift in behaviour noted at around 1 s^{-1}. This change in behaviour is likely due to initial breakup of weakly bound structure in the sample which occurs at low shear but is complete by the intermediate shear region. For example, in cement slurries, steep shear thinning is observed due to breakup of flocculated material [25]. Carbon black is known to agglomerate in water without stabilisation [26] so it is likely there are carbon black agglomerates present which disperse with shear.

The extracted power law coefficients are included in Table 1. The high shear parameters agree well with the extensional results, showing increasing consistency index (expected as viscosity increases) and decreasing power law coefficient in the order CMC, Alginate, Carrageenan, Guar. However, this does not capture the distinct difference in the behaviour of the Guar polymer (caused by the polymer branching) that is seen in extension and can be observed by the much higher critical time to breakup in the extensional models.

4. Conclusion

This work demonstrates that extensional rheology can vary hugely between battery slurry formulations and this cannot be captured by shear measurements. A rapid extensional rheometry measurement tool has been designed and implemented, and the extensional rheometry of 4 different binder systems measured. The results indicate excluding extensional measurements has a significant impact upon correctly understanding the slurry structure and flow properties. The data reported can be used to inform modelling approaches, as well as to validate physical models of electrode slurries, which must be able to correctly predict behaviour under extensional flow, in order to correctly predict flow in the coater and predict the final coating microstructure. The study of extensional rheology in electrode manufacturing will allow us to elucidate the microscale origins of the extensional rheology of battery slurries (e.g. study of different weight percentages, molecular weights of binder, addition of humidity control). This understanding is required to design novel slurries with optimal extensional properties for coating, which will allow precise design of the final coating microstructure. Quantifying the extension properties and of electrode slurries takes us a step further towards fully understanding the manufacturing process, implementing digital twins, and removing costly optimisation steps in industrial lines.

5. Data Availability

The raw/processed data required to reproduce these findings cannot be shared at this time as the data also forms part of an ongoing study.

CRediT authorship contribution statement

C.D. Reynolds: Conceptualization, Methodology, Data curation, Investigation, Formal analysis, Supervision, Writing – original draft. **J. Lam**: Data curation, Formal analysis, Investigation. **L. Yang**: Data curation, Formal analysis, Investigation. **E. Kendrick**: Supervision, Methodology, Funding acquisition, Writing – review & editing.

Declaration of Competing Interest

The authors declare that they have no known competing financial interests or personal relationships that could have appeared to influence the work reported in this paper.

Acknowledgments

The authors wish to thank Dr. Bart Hallmark and Prof. Ian Wilson at the University of Cambridge for providing the engineering drawings for Seymour which were used as basis for the 3D printed rheometer.

This work was funded by the Faraday Institution NEXTRODE project (faraday.ac.uk; EP/S003053/1, FIRG015), including a FUSE internship from the Faraday institution (FITG FUSE-064).

Materials & Correspondence

Requests for materials should be addressed to CDR

References

[1] Policy Paper: The Grand Challenges, Dep. Business, Energy Ind. Strateg. (2019). https://www.gov.uk/government/publications/industrial-strategy-the-grand-challenges/industrial-strategy-the-grand-challenges (accessed May 6, 2020).

[2] J. Ma, Y. Li, N.S. Grundish, J.B. Goodenough, Y. Chen, L. Guo, Z. Peng, X. Qi, F. Yang, L. Qie, C.-A. Wang, B. Huang, Z. Huang, L. Chen, D. Su, G. Wang, X. Peng, Z. Chen, J. Yang, S. He, X. Zhang, H. Yu, C. Fu, M. Jiang, W. Deng, C.-F. Sun, Q. Pan, Y. Tang, X. Li, X. Ji, F. Wan, Z. Niu, F. Lian, C. Wang, G.G. Wallace, M. Fan, Q. Meng, S. Xin, Y.-G. Guo, L.-J. Wan, The 2021 battery technology roadmap, J. Phys. D. Appl. Phys. 54 (18) (2021) 183001.

[3] R. Sommerville, P. Zhu, M.A. Rajaeifar, O. Heidrich, V. Goodship, E. Kendrick, A qualitative assessment of lithium ion battery recycling processes, Resour. Conserv. Recycl. 165 (2021) 105219.

[4] C.D. Reynolds, P.R. Slater, S.D. Hare, M.J.H. Simmons, E. Kendrick, A review of metrology in lithium-ion electrode coating processes, Mater. Des. 209 (2021) 109971, https://doi.org/10.1016/j.matdes.2021.109971.

[5] E. Kendrick, Advancements in Manufacturing, in: Futur. Lithium-Ion Batter, 2019: pp. 262–289.

[6] D. Gastol, M. Capener, C. Reynolds, C. Constable, E. Kendrick, Microstructural design of printed graphite electrodes for lithium-ion batteries, Mater. Des. 205 (2021) 109720, https://doi.org/10.1016/j.matdes.2021.109720.

[7] A. Yang, P. Salminen, S. Vervoort, I. Endres, H. Bachmann, Role of extensional viscosity in paper coating, Appl. Rheol. 21 (2011) 1–12, https://doi.org/10.3933/ApplRheol-21-23607.

[8] M. Schmitt, R. Diehm, P. Scharfer, W. Schabel, An experimental and analytical study on intermittent slot die coating of viscoelastic battery slurries, J. Coatings Technol. Res. 12 (2015) 927–938, https://doi.org/10.1007/s11998-015-9717-9.

[9] B. DG, The role of extensional rheology in polymer processing, Korea-Australia Rheol. J. 11 (1999) 305–311. http://www.cheric.org/research/tech/periodicals/view.php?seq=279834.

[10] B. Robertson, R.L. Thompson, T.C.B. McLeish, I. Robinson, Polymer extrudate-swell: From monodisperse melts to polydispersity and flow-induced reduction in monomer friction, J. Rheol. (N. Y. N. Y). 63 (2019) 319–333, https://doi.org/10.1122/1.5058207.

[11] L. Ouyang, Z. Wu, J. Wang, X. Qi, Q. Li, J. Wang, S. Lu, The effect of solid content on the rheological properties and microstructures of a Li-ion battery cathode slurry, RSC Adv. 10 (2020) 19360–19370, https://doi.org/10.1039/d0ra02651d.

[12] S. Lim, S. Kim, K.H. Ahn, S.J. Lee, The effect of binders on the rheological properties and the microstructure formation of lithium-ion battery anode slurries, J. Power Sources. 299 (2015) 221–230, https://doi.org/10.1016/j.jpowsour.2015.09.009.

[13] T.R. Tuladhar, M.R. Mackley, Filament stretching rheometry and break-up behaviour of low viscosity polymer solutions and inkjet fluids, J. Nonnewton. Fluid Mech. 148 (2008) 97–108, https://doi.org/10.1016/j.jnnfm.2007.04.015.

[14] G.H. Mckinley, T. Sridhar, Filament Stretching Rheometry of Complex Fluids, (2002) 375–415.

[15] G.H. McKinley, A. Tripathi, How to extract the Newtonian viscosity from capillary breakup measurements in a filament rheometer, J. Rheol. (N. Y. N. Y). 44 (2000) 653–670, https://doi.org/10.1122/1.551105.

[16] G.H. McKinley, Visco-elasto-capillary thinning and break-up of complex fluids, (2005).

[17] D.C. Vadillo, T.R. Tuladhar, A.C. Mulji, S. Jung, S.D. Hoath, M.R. Mackley, Evaluation of the inkjet fluid's performance using the "Cambridge Trimaster" filament stretch and break-up device, J. Rheol. (N. Y. N. Y). 54 (2010) 261–282, https://doi.org/10.1122/1.3302451.

[18] B. Hallmark, M. Bryan, E.d. Bosson, S. Butler, T. Hoier, O. Magens, N. Pistre, L. Pratt, B.-A. Ward, S. Wibberley, D.I. Wilson, A portable and affordable extensional rheometer for field testing, Meas. Sci. Technol. 27 (12) (2016) 125302.

[19] C. Collett, A. Ardron, U. Bauer, G. Chapman, E. Chaudan, B. Hallmark, L. Pratt, M. D. Torres-Perez, D.I. Wilson, A portable extensional rheometer for measuring the viscoelasticity of pitcher plant and other sticky liquids in the field, Plant Methods. 11 (2015), https://doi.org/10.1186/s13007-015-0059-5.

[20] L.E. Rodd, T.P. Scott, J.J. Cooper-White, G.H. McKinley, Capillary break-up rheometry of low-viscosity elastic fluids, Appl. Rheol. 15 (2005) 12–27, https://doi.org/10.1515/arh-2005-0001.

[21] K. Niedzwiedz, O. Arnolds, N. Willenbacher, R. Brummer, How to characterize yield stress fluids with capillary breakup extensional rheometry (CaBER)?, Appl Rheol. 19 (2009) 1–10, https://doi.org/10.3933/ApplRheol-19-41969.

[22] G.H. Mckinley, Visco-elasto-capillary thinning and break-up of complex fluids, Rheol. Rev. (2005) 1–48. http://www.bsr.org.uk.

[23] L.F. Zhao, Z. Hu, W.H. Lai, Y. Tao, J. Peng, Z.C. Miao, Y.X. Wang, S.L. Chou, H.K. Liu, S.X. Dou, Hard Carbon Anodes: Fundamental Understanding and Commercial Perspectives for Na-Ion Batteries beyond Li-Ion and K-Ion Counterparts, Adv. Energy Mater. 11 (2021) 1–75, https://doi.org/10.1002/aenm.202002704.

[24] D. Goeff, Q. Guo, Food Structure Development : The Interplay Between Processing Routes and Formulation Elements, Part A Food Struct, Dev. Interplay Between Process. Routes Formul. Elem. (2019) 1–28.

[25] D. Lootens, P. Hébraud, E. Lécolier, H. Van Damme, Gelation, Shear-Thinning and Shear-Thickening in Cement Slurries Solid/Liquid Dispersions in Drilling and Production Fluides chargés en forage et production pétrolière, Oil Gas Sci. Technol. IFP. 59 (1) (2004) 31–40.

[26] A. Basch, R. Horn, J.O. Besenhard, Substrate induced coagulation (SIC) of nano-disperse carbon black in non-aqueous media: The dispersibility and stability of carbon black in N-methyl-2-pyrrolidinone, Colloids Surfaces A Physicochem. Eng. Asp. 253 (2005) 155–161, https://doi.org/10.1016/j.colsurfa.2004.09.026.